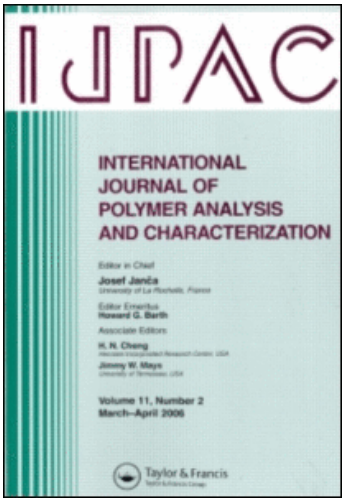

International Journal of Polymer Analysis and Characterization
Publication details, including instructions for authors and subscription information:
http://www.informaworld.com/smpp/title~content=t713646643

Biodegradable Poly(Lactic Acid)/Clay Nanocomposites by Melt Intercalation: A Study of Morphological, Thermal, and Mechanical Properties

Parakalan Krishnamachari[a]; Jian Zhang[a]; Jianzhong Lou[a]; Jizhong Yan[a]; Leonard Uitenham[a]
[a] Department of Mechanical and Chemical Engineering, North Carolina A&T State University, Greensboro, North Carolina, USA

To cite this Article Krishnamachari, Parakalan , Zhang, Jian , Lou, Jianzhong , Yan, Jizhong and Uitenham, Leonard(2009) 'Biodegradable Poly(Lactic Acid)/Clay Nanocomposites by Melt Intercalation: A Study of Morphological, Thermal, and Mechanical Properties', International Journal of Polymer Analysis and Characterization, 14: 4, 336 — 350
To link to this Article: DOI: 10.1080/10236660902871843
URL: http://dx.doi.org/10.1080/10236660902871843

International Journal of Polymer Anal. Charact., 14: 336–350, 2009

ISSN 1023-666X print
DOI: 10.1080/10236660902871843

Taylor & Francis
Taylor & Francis Group

Biodegradable Poly(Lactic Acid)/Clay Nanocomposites by Melt Intercalation: A Study of Morphological, Thermal, and Mechanical Properties

Parakalan Krishnamachari, Jian Zhang, Jianzhong Lou, Jizhong Yan, and Leonard Uitenham
Department of Mechanical and Chemical Engineering, North Carolina A&T State University, Greensboro, North Carolina, USA

Abstract: Biodegradable polymer nanocomposites of poly(lactic acid) (PLA) and several organically modified montmorillonites (nanoclays), namely, Cloisite 30B, Cloisite Na^+, Cloisite 25A, Cloisite 20A, Cloisite 93A, and Cloisite 15A were prepared by melt compounding using a Brabender twin-screw extruder. An exfoliated morphology was observed using both X-ray diffraction analysis (XRD) and transmission electron microscopy (TEM) for the combination of PLA and Cloisite 30B (the montmorillonite modified with a quaternary ammonium salt). The first XRD peaks for all the other nanocomposites were observed to shift to lower angles, indicating that intercalation occurred. The extent of intercalation depended on the type of organic modification on the Cloisite organoclay and was exhibited in the sequence of Cloisite $Na^+ > 25A > 20A > 93A > 15A$. Further studies were carried out to compare the properties of the PLA-30B nanocomposites with those of the neat PLA at clay loading levels of 1%, 2%, 3%, 4%, and 5% (w/w). Thermal stability of the nanocomposites was studied using thermogravimetric analysis (TGA). An increase in thermal stability was observed with a high at a loading level of 3% (w/w).

Submitted 15 December 2008; accepted 22 January 2009.

This work was partially funded by USDA Grant No. 2003-38820-14102 awarded to Dr. Lou and DOE Grant DE-FG26-06NT42742 awarded to Dr. Lou. One of the authors, Prof. Yan, was partially funded by the Visiting Scholarship from China.

Correspondence: Jianzhong Lou, Professor of Mechanical and Chemical Engineering, Department of Mechanical and Chemical Engineering, North Carolina A&T State University, 1601 E. Market St., Greensboro, NC 27411, USA. E-mail: lou@ncat.edu

Glass transition data were collected and analyzed using differential scanning calorimeter (DSC). An optimum in the glass transition temperature (T_g) of the nanocomposites was observed at 3% (w/w). Improvement in the mechanical properties of the nanocomposites was also observed.

Keywords: Biodegradable; Nanocomposite; Poly(lactic acid)

INTRODUCTION

In general, synthetic polymers that are produced from petrochemical products have low recovery/reproduction rates and are not easily degraded in the environment. The rapid growth of municipal waste drives efforts toward biocompatible/biodegradable polymers that can be used as renewable resources for polymer manufacturing and reduce the waste volume of plastics. Among various biodegradable polymers, poly(lactic acid) (PLA), a biodegradable aliphatic polyester, has attracted the most attention due to the fact that it can be derived from 100% renewable resources, such as corn and sugar beets. PLA is widely used in medical applications such as wound closure, surgical implants,[1] resorbable sutures,[2] tissue culture,[3] and controlled release systems.[4–7]

While biodegradable polymers are environmentally benign and are often produced from sustainable agricultural raw materials, the penetration of biodegradable polymers in the marketplace has encountered various barriers including cost and performance issues. For example, some of the properties such as brittleness, low heat distortion temperature, high gas permeability, and low melt viscosity for further processing restrict their use in a wide range of applications.[8] Therefore, modification of the biodegradable polymers through innovative technology is a formidable task for materials engineers.

The field of polymer nanocomposites, primarily based on layered silicates, such as montmorillonite (nanoclay), has drawn increasing attention from industry. The dispersion of the high-aspect-ratio nanoclay in the host polymers has been shown to impart substantial improvement on the mechanical, fire retardant, rheological, gas barrier, and optical properties, especially at low clay loading levels (as low as 1% (w/w)) in comparison with more conventional microcomposites (e.g., 30% (w/w) of microscale fillers).[9]

Many researchers have been involved in working on PLA nanocomposites. Sinha Ray et al.[10–13] extensively studied the effects of organic clay modifiers on the properties (biodegradability, melt rheology, etc.) of PLA-clay nanocomposites prepared by melt compounding with a twin screw extruder. Pluta et al.[14] compared the structure and several physical properties of PLA/clay nanocomposite loaded with organoclay and PLA/clay microcomposite containing sodium montmorillonite

prepared by melt compounding using a mixer. Ogata et al.[15] and Maiti et al.[16] have also reported on property enhancement of PLA through the addition of nanoclay.

There are three main techniques for preparing polymer nanocomposites: mixing the nanoclay with the monomer followed by polymerization (in situ polymerization),[17–19] mixing the nanoclay in the solution of a polymer followed by solvent evaporation (solution mixing),[20] and blending the nanoclay with a molten polymer (melt compounding).[21]

Recently, the melt compounding technique has become the method of choice because it is the most industrially viable approach that can lead to commercialized processes using existing infrastructure in the plastics industry. The absence of solvent makes it an economically and environmentally sound method. In this method, a dry mixture of the polymer pellets and the nanoclay powders is blended under shearing action of a twin screw, at a temperature above the melting point of the polymer. As a result of the organic modification, the clays are intercalated with alkyl ammonium cations bearing long alkyl chains, which increase the interlayer spacing and can improve the compatibility of nanoclay with the polymer matrix. The shearing action helps to facilitate the diffusion of the polymer chains from the bulk polymer melt into the galleries between the silicate layers of the nanoclay.[22]

The research in this study represents our most recent effort of preparing biodegradable nanocomposites of PLA and organically modified nanoclay by melt compounding using a Brabender twin-screw extruder. Several nanoclays were incorporated into PLA at 1% (w/w) loading level to form the nanocomposites. The morphology of the nanostructure was characterized using two complementary techniques: X-ray diffraction analysis (XRD) and transmission electron microscopy (TEM). Thermal stability of the nanocomposites was studied using thermogravimetric analysis (TGA). Glass transition temperature (T_g) data were collected and analyzed using differential scanning calorimetry (DSC). Mechanical properties of the nanocomposites were measured using the Instron universal testing machine. Improvement of the practical mechanical properties like mechanical property and thermal stability is compared with that of neat PLA. We also investigate the effect of nanoclay loading level on the T_g of the polymer nanocomposite.

EXPERIMENTAL SECTION

Materials

PLA under the commercial name PLA 4060D (poly-D/L-lactide or PDLLA) was supplied by NatureWorks (Minnetonka, Minn.). The resin

Table I. Nanoclay commercial names and surface treatments

Nanoclay	CEC (meq/100 g clay)	Surfactants
Cloisite® Na^+	92.6	None
Cloisite® 15A	125	$(HT)_2N^+(CH3)_2$
Cloisite® 20A	95	$(HT)_2N^+ (CH3)_2$
Cloisite® 25A	95	$(CH3)_2(C8H17)N^+(HT)$
Cloisite® 30B	90	$TN^+(CH3)(C2H4OH)_2$
Cloisite® 93A	90	$(HT)_2HN^+(CH3)$

HT = hydrogenated tallow amine; T = tallow amine.

was provided in the form of pellets. PLA 4060D has about 11 to 13% D-lactide content and a density of 1.24 g/cc.

The various grades of nanoclay, under the commercial names of Cloisite 30B, 15A, 20A, 25A, 93A, and Na^+ were supplied by Southern Clay Products Inc. (Gonzalez, Tex.). The surface treatment of the various nanoclay products is listed in Table I.

Nanocomposite Preparation

The pellets of PLA and the powders of the nanoclay were dry-mixed at room temperature followed by feeding into a C.W. Brabender twin-screw extruder. The melt temperature of the twin screw was maintained at 190°C. The rotation speed was set at 20 rpm. The Brabender twin screw extruder contains two 42 mm (1 5/8") diameter, counter-rotating (toward each other) intermeshing screws. The barrel of the extruder is equipped with two heater/cooler collar zones of 2300 watts each. There are a total of three temperature-controlled zones in the barrel in addition to the feeding zone.

Characterization

The morphology of the PLA-clay nanocomposites was studied using XRD and TEM. The interlay spacing d_{001} was examined using a Bruker D8 Discover Series 2 X-ray diffractometer. The measurements were carried out using reflection geometry and CuKα radiation (wavelength $\lambda = 0.154$ nm) operated at 40 kV and 100 mA. The d-spacing of clay in nanocomposites was calculated from Bragg's equation using the XRD results, which is the common procedure for polymer-clay nanocomposites.[23] TEM images were obtained using a Philips FEI CM12 electron microscope operated under 100 kV accelerating voltage

with a Gatan CCD camera. All samples were prepared with a diamond knife on a Leica Ultracut UCT microtome at room temperature to give sections with a nominal thickness of 70 nm.

Thermal analyses were carried out using DSC and TGA. A TA Instruments DSC Q100 was used to obtain the glass transition data. The samples were characterized in a temperature-modulated mode at a heating rate of 5°C/min in an inert atmosphere. A Perkin-Elmer TGA-7 was used for the thermogravimetric analysis at a heating rate of 5°C/min in an inert atmosphere from 40° to 600°C.

An Instron model 5566 Universal Testing Frame was used to measure the mechanical properties, including Young's modulus and ultimate tensile strength. The test was conducted at a constant rate of 2 inch/min at room temperature per ASTM D638 standard.

RESULTS AND DISCUSSION

Exfoliation in Melt Compounding

The XRD diffractograms for the PLA-clay nanocomposite samples of different clays are shown in Figure 1. The d-spacing information from the clay manufacturer is given in Table II. If the nanoclay retains its original layered structures and the original d-spacing when it is dispersed inside the polymer matrix, the position of the Bragg peak corresponding to the d-spacing in the XRD diffractogram will remain unchanged. If the layered structure is maintained and the d-spacing is increased, the Bragg

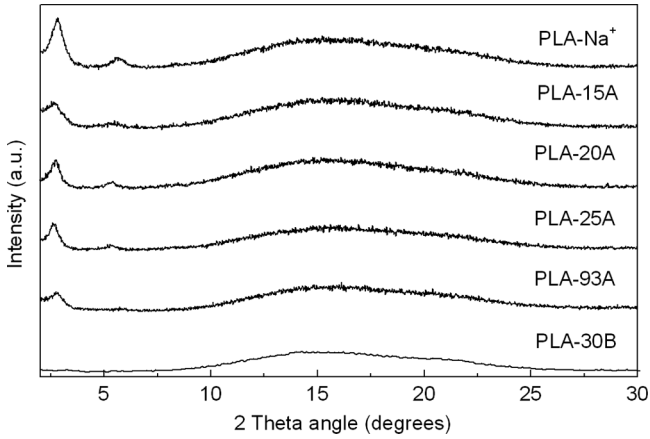

Figure 1. XRD diffractograms: PLA with 1% (w/w) of Na^+, 15A, 20A, 25A, 93A and 30B.

Table II. d-Spacing information for the nanoclays (Source: Southern clay products)

Nanoclay	d-spacing (nm)
Na^+	1.17
15A	3.15
20A	2.42
25A	1.86
93A	2.36
30B	1.8

peak will remain and it will be shifted to the left (lower 2θ value). If the layered structure is disrupted, the Bragg peak will disappear. It can be seen from Figure 1 that PLA-30B nanocomposite did not show a peak corresponding to the d-spacing of the nanoclay (30B). In contrast to the PLA-30B nanocomposite, the other PLA-nanoclay nanocomposites, namely PLA-Na^+, PLA-15A, PLA-20A, PLA-25A, and PLA-93A, were found to retain a Bragg peak corresponding to the clay d-spacing. It can be concluded that except for PLA-30B nanocomposite, none of the other PLA-nanoclay combinations achieved exfoliation. However, the first XRD peaks for all the other nanocomposites were observed to shift to lower angles, indicating that intercalation occurred. Krikorian and Pochan[24] also observed a similar phenomenon in their research with poly (L-lactic acid) nanocomposites.

The d-spacing of the nanoclay in the PLA nanocomposites was calculated from Bragg's equation:

$$d = \frac{n\lambda}{2\sin\theta}$$

where d is the spacing between layers of the clay, λ is the wavelength of the X-ray, which was equal to 0.154 nm, θ is the angle at the maximum point of the first peak (lowest θ) in the spectra, and n is a whole number, representing the order of diffraction, taken as one in our calculations. Table III summarizes the d-spacing values as calculated from the 2θ from the XRD measurement for the nanoclay and the PLA-nanoclay nanocomposites. It is apparent that the d-spacing values for the nanocomposites were greater than those of the nanoclay (data provided by the clay manufacturer in Table I), indicating an intercalated morphology when the polymer chains penetrated into the inter-gallery spaces to cause an increase in d-spacing. The extent of intercalation depended on the type of organoclay and was exhibited in the sequence of Cloisite Na^+ > 25A > 20A > 93A > 15A. It is interesting to note that the unmodified Cloisite Na^+ shows the highest increase in d-spacing. Lee

Table III. d-Spacing for the PLA-nanoclay nanocomposites

PLA-nanoclay nanocomposites	2θ	d-spacing (nm)
PLA-Na^+	2.8	3.15
PLA-15A	2.66	3.31
PLA-20A	2.7	3.26
PLA-25A	2.62	3.36
PLA-93A	2.78	3.17
PLA-30B	None	None

et al.[25] also observed a similar sequence in their research with tapioca starch-poly (lactic acid)-based nanocomposites.

In Figure 2, the XRD diffractograms of the nanoclay 30B and PLA-30B nanocomposites with 1%, 2%, and 3% (w/w) of 30B are compared. The Bragg peak for the 30B nanoclay (without polymer) was located at $2\theta = 4.9°$, which corresponds to the d-spacing of $d_{001} = 1.8\,\text{nm}$. The control sample of PLA (without nanoclay, but subjected to the same twin-screw extrusion process), labeled as 0%-30B, showed only the background scattering with low intensity. For the PLA-30B nanocomposites of different nanoclay loading levels, there were no noticeable XRD peaks of 30B observed at low-angle range, confirming that the exfoliation of silicate layers of 30B in the PLA matrix was obtained as a

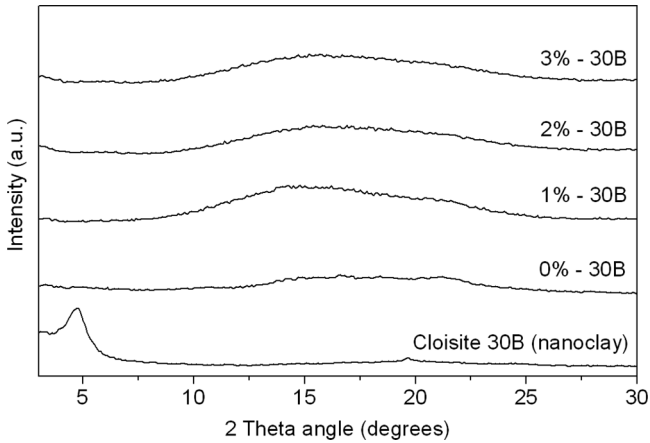

Figure 2. XRD Diffractograms: Cloisite 30B and PLA with 0%, 1%, 2% and 3% (w/w) of Cloisite 30B. Notice that there is no evidence of a nanoclay (30B) d-spacing peak for all nanocomposite compositions.

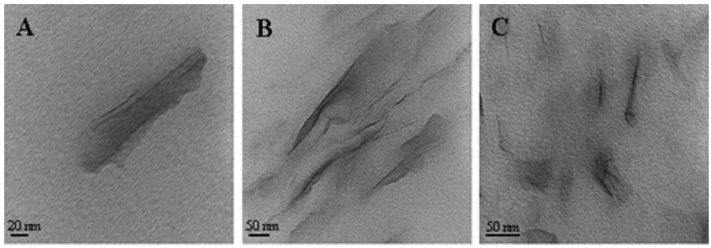

Figure 3. TEM Images: 2% 30B (w/w) in PLA (A), 3% 30B (w/w) in PLA (B) and 5% 30B (w/w) in PLA (C).

result of melt compounding. This lack of inter-gallery clay diffraction is due to the disorderly and random distribution of the clay platelets within the PLA matrix.

Following the observations from the XRD study, TEM analysis was done on the PLA-30B nanocomposite to visualize the clay dispersion on the nanoscale. Selected TEM images of the PLA-30B nanocomposite (2%, 3%, and 5% (w/w) of nanoclay 30B) are shown in Figure 3. It is generally observed that the extent of exfoliation is not necessarily a function of the loading level of the nanoclay 30B. The TEM images displayed here were selected out of several images of various magnifications over two or three sections of each sample to ensure that analysis was based on a representative region of the sample. While there are areas of exfoliation, there are regions in the images where tactoids of nanoclay are visible, indicating that the exfoliation was not as complete as we desired.

Following this morphological study, DSC, TGA, and mechanical property studies were done only on the PLA-30B nanocomposites with varying loading levels of the nanoclay 30B.

Thermal Analyses

The DSC thermograms of the PLA-30B nanocomposites are shown in Figure 4 and the values for the T_g in Table IV. The T_g increased by the addition of the 30B nanoclay. The T_g of the control sample of PLA (labeled 0%-30B in Figure 4) is 47.4°C. An increase of 6°C was observed by the addition of 1% 30B. At a loading level of 3% (w/w), the T_g is 51.4°C, which is still higher than that of the control sample of PLA but lower than that of the T_g of the 2%-30B sample.

The glass transition is a complex phenomenon depending on a number of factors such as chain flexibility, molecular weight, branching, cross-linking, intermolecular interactions, and steric effects.[26,27] The

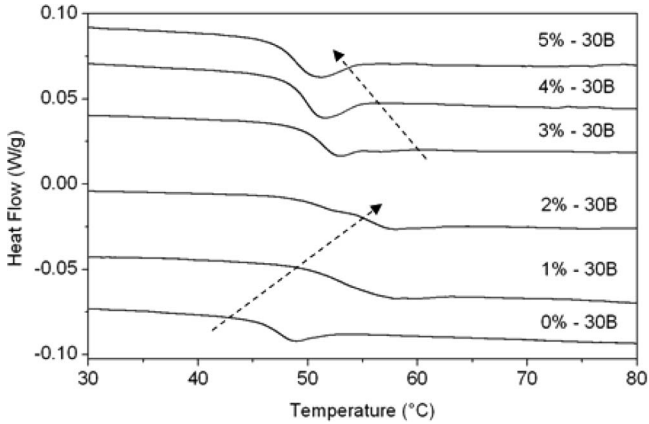

Figure 4. DSC thermograms for PLA with 0%, 1%, 2%, 3%, 4% and 5% (w/w) of Cloisite 30B. PLA with 0%-30B denotes the control sample of PLA. Experiments carried out in a temperature-modulated DSC operated at heating rate of 5°C/min. Arrows indicate the trend of the T_g.

increase in T_g at the lower loading levels of the nanoclay 30B could be attributed to the decrease in free volume in the polymer matrix due to the cross-linkings caused by the *hydrogen bond* between the diols of the organic modifier of the nanoclay (Cloisite 30B) and the carbonyl group (C=O) in the PLA.[24] If the surface of the organically modified nanoclay has a favorable interaction with the polymer chains, it should help *immobilize* the polymer chains that are adjacent to the clay surface and thus cause an increase in T_g.

The decrease in T_g by the addition of the nanoclay has also been observed by Lee et al.[28] At higher loading levels it is likely that the population of the nanoclay particles is large enough to provide steric effects that prevent the chains from packing compactly. This could increase the free volume of the polymer matrix and lead to the

Table IV. T_g values of various PLA-30B nanocomposites

Nanocomposite (PLA-30B)	Glass transition temperature (°C)
0%-30B (control of PLA)	47.4
1%-30B	53.2
2%-30B	55.2
3%-30B	51.3
4%-30B	49.9
5%-30B	48.9

decrease in T_g. It is also possible that the plasticizing effects of the organic modifier used for the nanoclay becomes significant at higher loading levels. Xu et al.[29] also observed this trend of limiting factor in their research with PVC nanocomposites. Zhu and Wool[30] observed a similar phenomenon in their research with nanoclay reinforced bio-based elastomers. While on one hand the clay bundles restrict the molecular motions and enhance the T_g, on the other hand the organic modifier has the potential to bring some plasticizer effects to reduce the T_g.

Optimization of the loading levels in a filled polymer is very critical. In conventional fillers (micro fillers) it is generally observed that the addition of filler beyond the optimum limit leads to an increase of the filler-filler interaction instead of the more desirable filler-matrix interaction.[31] An increase of these filler-filler interaction beyond the optimum limit will lead to formation of aggregates. Ismail et al.[32] in their research with fillers for natural rubber compounds also found out that aggregation of the filler particles leads to a reversal in the properties of the filled polymer. The over-population of the filler leading to agglomeration is observed in the nanocomposites also. It has been reported[33,34] that even nanoclays have the tendency to form aggregates when their loading is beyond a certain level.

An increase in thermal stability with the increase in nanoclay loading level was observed from the TGA traces, as shown in Figure 5, with a high obtained for a loading of 3% (w/w). This increase in thermal stability could be attributed to an ablative reassembling of the silicate

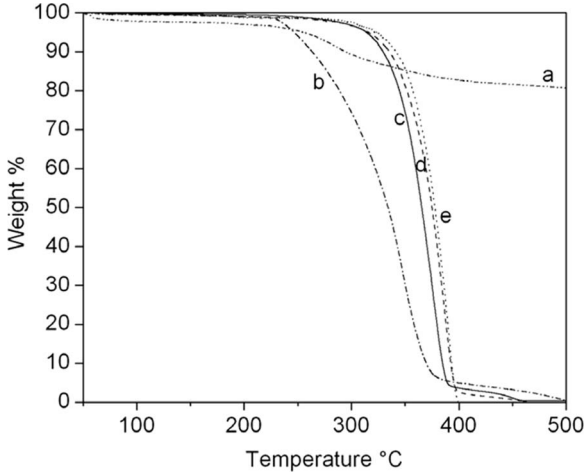

Figure 5. The TGA thermograms of Cloisite 30B (a) and PLA with 0% (b), 1% (c), 2% (d) and 3% (e) (w/w) of Cloisite 30B. Tests conducted at heating rate of 5°C/ min under inert conditions from 40°C to 600°C.

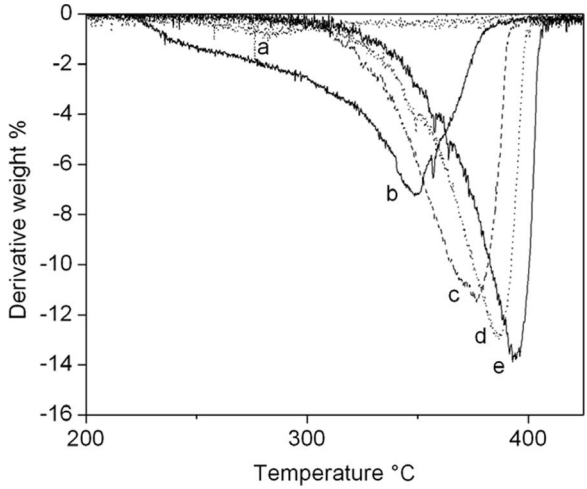

Figure 6. Derivative weight loss from TGA for Cloisite 30B (a) and PLA with 0% (b), 1% (c), 2% (d), and 3% (e) (w/w) of Cloisite 30B. Note that the weight loss in the curve (a) – Cloisite 30B is due to the loss of the surface modifier of the nanoclay.

layers, which may occur on the surface of the nanocomposites, creating a protective physical barrier. In addition, the decomposition might also be delayed by the labyrinth effect of the silicate layers exfoliated in the nanocomposites.[35]

The d-TGA curves (derivative weight loss curves) are a fair indication of the temperature at which the maximum weight loss is triggered (see Figure 6 and Table V). It was observed that there was a shift towards the positive direction with the increase in the loading levels of the nanoclay. The increase in thermal stability could also be attributed to the high thermal stability of clay and to the favorable interactions between the surface of nanoclay particles and the polymer matrix.[36–38]

Table V. Temperature at which maximum weight loss occurred for PLA-30B nanocomposites

Nanocomposite (PLA-30B)	Temperature at max weight loss (°C)
Cloisite 30B	281.4
0%-30B (control of PLA)	349.3
1%-30B	376.7
2%-30B	386.3
3%-30B	393.8

Table VI. Mechanical properties of PLA and PLA-30B nanocomposite

Property	0%-30B (Control of PLA)	1%-30B (PLA-30B nanocomposite)
Ultimate tensile strength (MPa)	34.0	38.0
Young's modulus (GPa)	0.81	0.94

Mechanical Properties

An Instron model 5566 Universal Testing Frame was used to measure the tensile properties for the PLA-30B nanocomposites. The tests were conducted at a constant rate of 2 inch/min in room temperature under ASTM D638 standard. In Table VI, the property of the control of PLA was compared with the nanocomposite of 1% (w/w) of 30B. There was an increase in the mechanical properties of the PLA-30B nanocomposite compared to the unfilled PLA.

CONCLUSION

Polymer nanocomposites of biodegradable PLA and organically modified nanoclay were prepared by melt compounding using a Brabender twin-screw extruder. An exfoliated morphology was achieved for PLA-Cloisite 30B as evidenced by XRD and TEM measurement and an intercalated morphology for the other Cloisite nanoclays. The extent of intercalation depended on the type of organic modification on the Cloisite organoclay and was exhibited in the sequence of Cloisite $Na^+ > 25A > 20A > 93A > 15A$. Further studies were done on the PLA-Cloisite 30B nanocomposite. An increase in thermal stability was observed by TGA, with a high obtained at a clay loading level of 3% (w/w). T_g measured by DSC also showed an increase. There was a reversal in the trend at higher clay loading levels. There was a decrease in the T_g above 3% (w/w). Improvement in the mechanical properties of the nanocomposites was also observed.

REFERENCES

[1] Taylor, M. S., A. U. Daniels, K. P. Andriano, and J. Heller. (1994). Six bioabsorbable polymers: *In vitro* acute toxicity of accumulated degradation products. *J. Appl. Biomater.* **5**(2), 151–157.

[2] Jain, R. A. (2000). The manufacturing techniques of various drug loaded biodegradable poly(lactide-co-glycolide) (PLGA) devices. *Biomaterials* **21**(23), 2475–2490.

[3] Mikos, A. G., M. D. Lyman, L. E. Freed, and R. Langer. (1994). Wetting of poly(-lactic acid) and poly(-lactic-co-glycolic acid) foams for tissue culture. *Biomaterials* **15**(1), 55–58.
[4] Park, T. G., S. Cohen, and R. Langer. (1992). Poly(L-lactic acid)/pluronic blends: Characterization of phase separation behavior, degradation, and morphology and use as protein-releasing matrixes. *Macromolecules* **25**(1), 116–122.
[5] Kamath, K. R., and K. Park. (1993). Biodegradable hydrogels in drug delivery. *Adv. Drug Deliv. Rev.* **11**(1–2), 59–84.
[6] Davis, S. S., L. Illum, and S. Stolnik. (1996). Polymers in drug delivery. *Curr. Opin. Colloid Interface Sci.* **1**(5), 660–666.
[7] Edlund, U., and A. Albertsson. (2002). Degradable polymer microspheres for controlled drug delivery. In *Degradable Aliphatic Polyesters*. Berlin: Springer.
[8] Sinha Ray, S., K. Yamada, M. Okamoto, Y. Fujimoto, A. Ogami, and K. Ueda. (2003). New polylactide/layered silicate nanocomposites. 5. Designing of materials with desired properties. *Polymer* **44**(21), 6633–6646.
[9] Alexandre, M., and P. Dubois. (2000). Polymer-layered silicate nanocomposites: Preparation, properties and uses of a new class of materials. *Mater. Sci. Eng. R Rep.* **28**(1–2), 1–63.
[10] Sinha Ray, S., P. Maiti, M. Okamoto, K. Yamada, and K. Ueda. (2002). New polylactide/layered silicate nanocomposites. 1. Preparation, characterization, and properties. *Macromolecules* **35**(8), 3104–3110.
[11] Sinha Ray, S., K. Yamada, M. Okamoto, and K. Ueda. (2003). New polylactide-layered silicate nanocomposites. 2. Concurrent improvements of material properties, biodegradability and melt rheology. *Polymer* **44**(3), 857–866.
[12] Sinha Ray, S., K. Yamada, M. Okamoto, A. Ogami, and K. Ueda. (2003). New polylactide/layered silicate nanocomposites. 3. High-performance biodegradable materials. *Chem. Mater.* **15**(7), 1456–1465.
[13] Sinha Ray, S., and M. Okamoto. (2003). New polylactide/layered silicate nanocomposites, 6. *Macromol. Mater. Eng.* **288**(12), 936–944.
[14] Pluta, M., A. Galeski, M. Alexandre, M. A. Paul, and P. Dubois. (2002). Polylactide/montmorillonite nanocomposites and microcomposites prepared by melt blending: Structure and some physical properties. *J. Appl. Polym. Sci.* **86**(6), 1497–1506.
[15] Ogata, N., G. Jimenez, H. Kawai, and T. Ogihara. (1997). Structure and thermal/mechanical properties of poly(*l*-lactide)-clay blend. *J. Polym. Sci. Part B Polym. Phys.* **35**(2), 389–396.
[16] Maiti, P., K. Yamada, M. Okamoto, K. Ueda, and K. Okamoto. (2002). New polylactide/layered silicate nanocomposites: Role of organoclays. *Chem. Mater.* **14**(11), 4654–4661.
[17] Usuki, A., Y. Kojima, M. Kawasumi, A. Okada, Y. Fukushima, T. Kurauchi, and O. Kamigaito. (1993). Synthesis of nylon 6-clay hybrid. *J. Mater. Res.* **8**, 1179–1184.
[18] Kojima, Y., A. Usuki, M. Kawasumi, A. Okada, Y. Fukushima, T. Kurauchi, and O. Kamigaito. (1993). Mechanical properties of nylon 6-clay hybrid. *J. Mater. Res.* **8**, 1185–1189.

[19] Gaboune, A., S. Sinha Ray, A. AitKadi, B. Riedl, and M. Bousmina. (2006). Polyethylene/clay nanocomposites prepared by polymerization compounding method. *J. Nanosci. Nanotechnol.* **6**, 530–535.
[20] Aranda, P., and E. Ruiz-Hitzky. (1992). Poly(ethylene oxide)-silicate intercalation materials. *Chem. Mater.* **4**(6), 1395–1403.
[21] Vaia, R. A., H. Ishii, and E. P. Giannelis. (1993). Synthesis and properties of two-dimensional nanostructures by direct intercalation of polymer melts in layered silicates. *Chem. Mater.* **5**(12), 1694–1696.
[22] Vaia, R. A., and E. P. Giannelis. (1997). Polymer melt intercalation in organically-modified layered silicates: Model predictions and experiment. *Macromolecules* **30**(25), 8000–8009.
[23] Sperling, L. H. (2001). *Introduction to Physical Polymer Science*. New York: Wiley-Interscience.
[24] Krikorian, V., and D. J. Pochan. 2003. Poly(L-lactic acid)/layered silicate nanocomposite: Fabrication, characterization, and properties. *Chem. Mater.* **15**(22), 4317–4324.
[25] Lee, S. Y., Y. X. Xu, and M. A. Hanna. (2007). Tapioca starch-poly (lactic acid)-based nanocomposite foams as affected by type of nanoclay. *Int. Polym. Process.* **22**(5) 429–435.
[26] Cowie, J. M. G. (1991). *Polymers: Chemistry & Physics of Modern Materials*. New York: Chapman & Hall.
[27] Clegg, D. W., and A. A. Collyer, eds. (1986). *Mechanical Properties of Reinforced Thermoplastics*. London: Elsevier, p. 2.
[28] Lee, J. H., T. G. Park, H. S. Park, D. S. Lee, Y. K. Lee, S. C. Yoon, and J.-D. Nam. (2003). Thermal and mechanical characteristics of poly(-lactic acid) nanocomposite scaffold. *Biomaterials* **24**(16), 2773–2778.
[29] Xu, W., Z. Zhou, M. Ge, and W. P. Pan. (2004). Polyvinyl chloride/montmorillonite nanocomposites: Glass transition temperature and mechanical properties. *J. Therm. Analy. Calorim.* **78**, 91–99.
[30] Zhu, L., and R. P. Wool. (2006). Nanoclay reinforced bio-based elastomers: Synthesis and characterization. *Polymer* **47**(24), 8106–8115.
[31] Azura, A. R., S. Ghazali, and M. Mariatti. (2008). Effects of the filler loading and aging time on the mechanical and electrical conductivity properties of carbon black filled natural rubber. *J. Appl. Polym. Sci.* **110**(2), 747–752.
[32] Ismail, H., M. N. Nasaruddin, and H. D. Rozman. (1999). The effect of multifunctional additive in white rice husk ash filled natural rubber compounds. *Eur. Polym. J.* **35**(8), 1429–1437.
[33] Yasmin, A., J. L. Abot, and I. M. Daniel. (2003). Processing of clay/epoxy nanocomposites by shear mixing. *Scr. Mater.* **49**(1), 81–86.
[34] Lam, C.-K., H.-Y. Cheung, K.-T. Lau, L.-M. Zhou, M.-W. Ho, and D. Hui. (2005). Cluster size effect in hardness of nanoclay/epoxy composites. *Composites Part B Engineering* **36**(3), 263–269.
[35] Gilnian, J. W., T. C. L. Kashivagi, E. P. Giannelis, E. Manias, S. Lomakin, and J. D. Lichtenhan. (1998). *Fire Retardancy of Polymers*. Cambridge: Royal Society of Chemistry.

[36] Wen, J., and G. L. Wilkes. (1996). Organic/inorganic hybrid network materials by the sol-gel approach. *Chem. Mater.* **8**(8), 1667–1681.
[37] Fischer, H. R., L. H. Gielgens, and T. P. M. Koster. (1999). Nanocomposites from polymers and layered minerals. *Acta Polym.* **50**(4), 122–126.
[38] Petrović, Z. S., I. Javni, A. Waddon, and G. Bánhegyi. (2000). Structure and properties of polyurethane-silica nanocomposites. *J. Appl. Polym. Sci.* **76**(2), 133–151.